ELSEVIER

Thin Solid Films 422 (2002) 141–149

thin solid films

www.elsevier.com/locate/tsf

Ion solid surface interactions in ionized copper physical vapor deposition

X.-Y. Liu[a,*], M.S. Daw[b,1], J.D. Kress[c], D.E. Hanson[c], V. Arunachalam[b], D.G. Coronell[b,2], C.-L. Liu[d], A.F. Voter[c]

[a]*Computational Nanoscience Group, Physical Sciences Research Laboratories, Motorola, Inc., Los Alamos, NM 87545, USA*
[b]*Digital DNA Laboratories, Motorola, Inc., Austin, TX 78721, USA*
[c]*Theoretical Division, Los Alamos National Laboratory, Los Alamos, NM 87545, USA*
[d]*Digital DNA Laboratories, Motorola, Inc., Mesa AZ 85202, USA*

Received 23 July 2002; received in revised form 23 July 2002; accepted 13 September 2002

Abstract

A thorough understanding of ion-solid surface interactions is important for the predictive modeling of ionized metal plasma (IMP) Cu physical vapor deposition (PVD) at feature scales. Besides sticking coefficients and sputter yields, characterizations such as angular distributions of sputtered and reflected particles, and thermal-accommodation coefficients are also needed as inputs for a feature scale process simulator. Molecular dynamic (MD) simulations have been used to provide pertinent information and physical insights. MD results for Ar^+/Cu and Cu^+/Cu systems as a function of hyperthermal ion energies and incidence angles are reported. The issue of integrating different sticking coefficients for different surface roughness is addressed, based on ion travel distance analysis. We have found that the angular distribution of sputtered particles is not cosine, but can be described by a simple Gaussian-like formula. Ion reflection characteristics are also analyzed.
© 2002 Elsevier Science B.V. All rights reserved.

Keywords: Copper; Molecular dynamics

1. Introduction

In recent years, Cu has been considered to replace Al as interconnect materials for advanced ultra-large scale integrated (ULSI) circuits metallization in semiconductor device manufacturing processes. Ionized metal plasma (IMP) physical vapor deposition (PVD) has played a critical role in the ability to deposit conformal Cu films over features such as dual inlaid structures [1,2]. Historically, PVD has been widely used for blanket metal film deposition, but it is impractical for high aspect ratio trenches and bias. For high aspect ratio interconnect features [3,4], IMP-PVD has been found to be a superior technique for depositing films. This process is characterized by a highly directional ion flux through an inductively coupled RF plasma, with the ions accelerated towards the substrate by a DC bias. IMP-PVD is a significantly more complex process than conventional PVD, which challenges the modeling and simulation of the process. The ions (Cu^+ and Ar^+) that are accelerated towards the substrate have a distribution of energies and angles, which affects their interaction with the surface. For conventional PVD processes, the surface interactions are adequately described by a constant sticking coefficient that is independent of incidence angle or energy. In IMP-PVD, however, this is not the case, and a detailed understanding of the ion solid surface interaction is needed for accurate feature scale modeling of the process [1,2,5]. In this paper, we review our research activity on the modeling of ion solid surface interactions in IMP Cu PVD based on molecular dynamics (MD) simulations.

Historically, MD simulations of sputtering of solid surfaces have been predominantly in the energy range of 1 keV or above. More recently, a number of MD simulations were carried out at hyperthermal ion ener-

*Corresponding author. Tel.: +1-505-663-5130; fax: +1-505-663-5150.
E-mail address: r40298@motorola.com (X.-Y. Liu).
[1] Present address: Department of Physics and Astronomy, Clemson University, Clemson, SC 29634, USA.
[2] Present address: Reaction Design, 6440 Lusk Blvd., Suite D-209, San Diego, CA 92121, USA.

0040-6090/02/$ - see front matter © 2002 Elsevier Science B.V. All rights reserved.
PII: S0040-6090(02)00870-2

gies, i.e. 1 eV to 100 eV, which we briefly review here. The results of MD simulations using pair potentials have been used to analyze the experimental angle-resolved, time-of-flight distributions of Ar atoms emitted during Ar+ bombardment of Cu surfaces for energies of a few keV down to 200 eV [6]. MD calculations of normal incidence sticking probability and penetration depth were carried out for Cu on Cu(100) and (111) surfaces with pair potentials [7]. Energy deposition, reflection and sputtering for hyperthermal rare-gas atoms impacting Cu were studied with MD simulations [8]. MD simulations of Ar ion interactions with Si surfaces have been carried out to obtain the sputter yield and formation pathways in the ion energy range from 25 to 200 eV [9]. Energetic ion (100 and 200 eV) bombardment of SiO_2 surfaces has been studied with MD simulations [10]. Also, sticking probability, penetration depth, and emission characterization for Cu atoms deposited on the Cu(100) surfaces have been studied with effective pair potential in MD simulations of thin film deposition [11].

We have previously reported MD simulations of Cu and Ar ion sputtering of Cu(111) surfaces using the embedded atom method (EAM) potential for ion energies in the range of 10–100 eV [12]. The calculated energy and angle dependent sputter yields, sticking coefficients, etc., can then be implemented in a feature scale topographic profile simulator, as was demonstrated for Cu ionized PVD [5]. Similar calculations have been performed for Ni and Al surfaces [13]. Additionally, the mechanism of trapping and desorption of energetic Cu atoms on Cu(111) surfaces at grazing incidence has been studied [14]. Similar to our work, sticking coefficients and three-dimensional spatiokinetic distributions of sputtered and scattered products of Ar^+ and Cu^+ impacting amorphous Cu surfaces have been determined with MD simulations using EAM potentials [15,16]. Also, similar MD simulations were done for Ar^+ and Al^+ impacting Al(111) surfaces [17,18]. Compared with our previous MD simulations [5,12], we believe the results presented here are more accurate since they are derived from a much larger set of MD simulation runs.

As described in Arunachalam et al. [1,2], the feature scale profile simulation is based on a Monte Carlo particle moving approach. The ion surface interaction parameters obtained from MD simulations are used as inputs to the feature scale simulator, a schematic of which is shown in Fig. 1. When the ions impact the surface, they may adsorb or reflect based on the value of the sticking coefficient. This model requires the following ion surface interaction parameters: (1) sticking coefficient; (2) sputter yield; (3) thermal accommodation coefficient (TAC); (4) sputtered particle angular distribution; and (5) reflected particle angular distribution. TAC is defined as $(E_{inc}-E_{refl})/(E_{inc}-E_0)$, where E_{inc} is the incident particle energy, E_{refl} is the reflected particle energy, and E_0 is kT, where k is Boltzmann's constant and T is absolute temperature (we used 300 K in calculations). These interaction parameters are obtained from atomistic MD simulations, which are to be discussed in this paper.

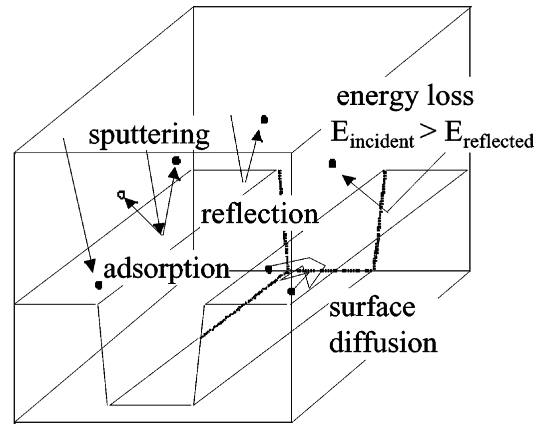

Fig. 1. Schematic of the feature scale simulation.

2. Description of simulation

For our MD simulations, we used a combined EAM potential (see Kress et al. [12] for details) for the Cu–Cu interactions [19] with the universal Ziegler–Biersack–Littmark (ZBL) pair potential [20] for Ar–Cu and the Molière pair potential [21] for Ar–Ar. Although we are studying ion sputtering, a neutral-atom potential such as EAM is appropriate because the incident ion is neutralized well before impact by a fast Auger process or resonant charge transfer [22]. Therefore, any reference to an ion in this work actually corresponds to a neutral Cu atom in the simulation. The EAM potential is known to be generally reliable for predicting metallic properties, given carefully constructed interatomic potentials. The Cu potential used here was fit to experimental properties of the bulk solid and gas-phase diatomic molecule. The repulsive wall of this EAM potential agrees well with density functional B3LYP Gaussian calculations for a Cu dimer up to 100 eV.

The MD simulation substrate has 972 Cu atoms arranged as a fcc crystal of 12×9×9 atoms (x,y,z) with periodic boundary conditions imposed along the x and y axes (periods = 23.00 Å and 26.56 Å, respectively) and a free (111) surface normal to the z axis. The simulation method is similar to that used in MD simulations of Cl ion etching of Si [23]. The Cu(111) substrate lattice and the periodic boundary lengths were first rescaled according to the thermal expansion of Cu bulk determined from a constant pressure MD simulation. Then the substrate was thermally annealed at 300 K for 0.5 ns to reach equilibrium. Sputtering simulations began with a Cu or Ar ion at a random x, y position, just inside the cut-off distance of the potential energy

function, which was approximately 5 Å above the surface. The components of the ion velocity were chosen to yield the desired energy and angle with respect to the surface normal; the azimuthal angle was chosen randomly. The bottom two layers (216 atoms) of the substrate were rigidly fixed. For each incidence angle and energy, a series of 450 impact events were run as five sets of 90 events, using constant energy MD. At the end of the series, the statistical average and standard deviation from these 5 cases were computed to obtain results.

The equations of motion were integrated using the leap-frog Verlet method with 2.5 fs time step and no thermostat. For Cu impacts, the integration times of MD were as follows: 1 ps for incidence angle from 0° to 45°, 3 ps for incidence angle from 50° to 65°, and 5 ps for incidence angle from 70° to 85°. The integration times increased with larger impact angles because the Cu impact atom at oblique angles can travel large distance on the surface before sticking or desorbing. For Ar impacts, an integration time of 1 ps was used. Since ions may travel long distance outside the simulation box because of their large velocities, special care was taken to ensure that the periodic boundary conditions were maintained throughout the simulation period.

The sputter yield is defined as the number of surface atoms ejected per incident ion. The sticking coefficient is the probability that the incident ion remains bound to the surface throughout the MD simulation period. To check size effects, simulations of surface area four times larger or substrate two times thicker have been done. The sticking coefficient results agree within statistical accuracy. Another check shows that the sticking coefficient change was insensitive to the use of a thermostat (Langevin dynamics) to dissipate energy deposited during impact.

For simulations on a non-crystalline surface, the initial Cu surface was 'amorphized' by thermal annealing to a melting temperature followed by a rapid quenching (as prescribed by Abrams and Graves [15]). We then annealed this non-crystalline surface sample at 300 K for 5 ps. The final equilibrated surface was then used as the substrate in our MD simulations.

3. Results and discussions

3.1. Sticking coefficient

The interaction potential between Ar and Cu atoms is purely repulsive, so the sticking coefficients are expected to be zero for Ar ions on Cu substrate. We find that this is indeed true in our simulation results of Ar ion impacting the Cu(111) surface. The Ar ions have zero sticking probability in the ion energy range from 10 to 125 eV, with incidence angles from 0° (normal incidence) to 85°. At higher energies, a small number of Ar ions may penetrate deeply into Cu bulk and become trapped. For example, for 250 eV ion energy at normal incidence, approximately 13% Ar ions are trapped in the Cu bulk.

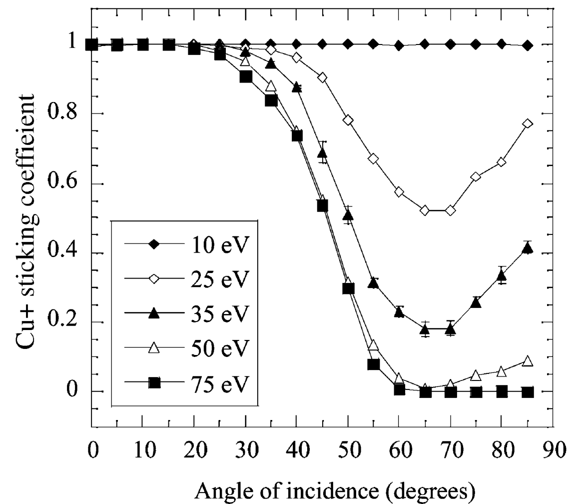

Fig. 2. Sticking coefficient as a function of angle of incidence and energy for Cu^+ impacting a Cu(111) surface. Error bars are shown for the 35 eV case.

For Cu^+/Cu interactions, the results are more complicated. Fig. 2 shows the sticking probability vs. angle of incidence for Cu ion impacting a Cu(111) surface predicted by MD simulations for ion energies between 10 and 75 eV (for ions of 100 eV in energy, the sticking coefficient result is nearly identical to that of ions at 75 eV, and thus the data were not plotted for clarity). At 10 eV, the sticking coefficient is unity for all incidence angles. Above 10 eV, the sticking coefficient starts to decrease from unity when the incidence angles are off-normal. At 75 eV, the sticking coefficient changes monotonically from unity to zero as the angle of incidence increases. Between 10 and 50 eV, the sticking coefficient decreases as the angle of incidence increases for angles up to 65°. Above 65°, the sticking coefficient increases up to grazing incidence (near 90°). The result here confirms our previous finding of this phenomenon [5,12]. The reason for the upturn of the sticking coefficient at high incidence angles is discussed in more detail in Hanson et al. [14]. For Cu ions impacting the Cu(111) surface at near grazing incidence, the ions can become trapped by the mean attractive potential above the surface, oscillating normal to the surface. In this trapped state, the ions traverse hundreds of angstroms as they dissipate energy to the surface.

It is useful to analyze quantitatively the total distance traversed by a Cu^+ at the surface. Fig. 3a shows this average distance for adsorbed Cu^+ on the Cu(111) surface for different ion energies as a function of incidence angle. Fig. 3b shows the corresponding probability distribution in each case for incidence angles from 50° to 85°, with the ion energy at 25 eV. From

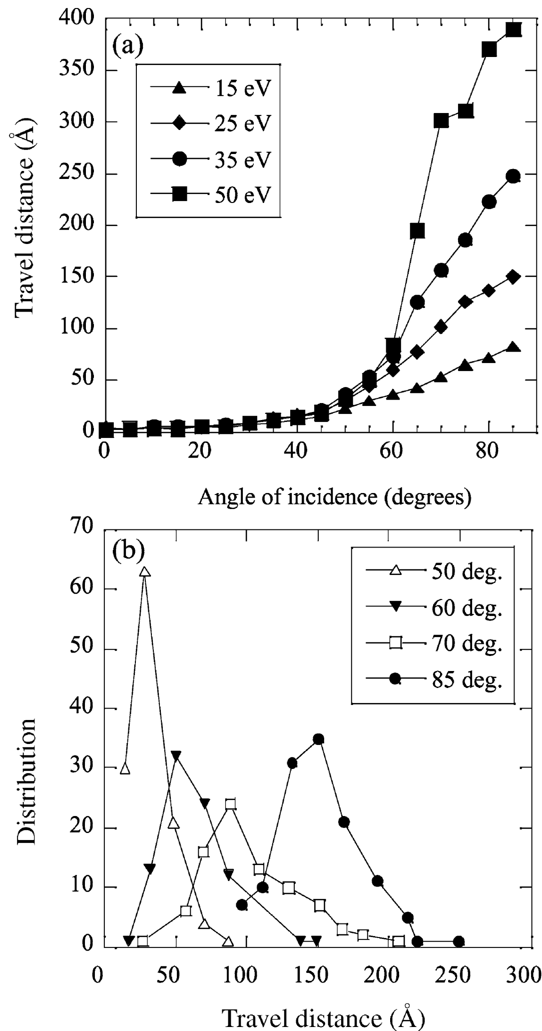

Fig. 3. (a) The average distance traversed by a Cu^{+} on Cu(111) before being adsorbed. (b) The distance distribution for 25 eV ions.

these plots, we conclude that the distance traversed by ions impacting Cu(111) surface at incidence angle from 70° and larger will likely be more than 100 Å. An accurate measurement of surface smoothness dimensions under IMP-PVD conditions is not available currently, but we tend to propose that the assumption of a smooth Cu(111) substrate is valid for distances of a few tens of angstroms. Near grazing incidence, sputtering may occur via collisions with step edge and the sticking coefficients obtained using a smooth (111) surface may not be applicable to modeling IMP deposition, thus, making surface morphology important in sputtering simulations.

To examine the role of surface morphology, we performed MD sputtering simulations for a non-crystalline (amorphous-like) Cu surface. Fig. 4 shows the sticking coefficients for the amorphous surface. The amorphous surface sticking coefficient results show no upturn at near grazing incidence angles, in contrast to

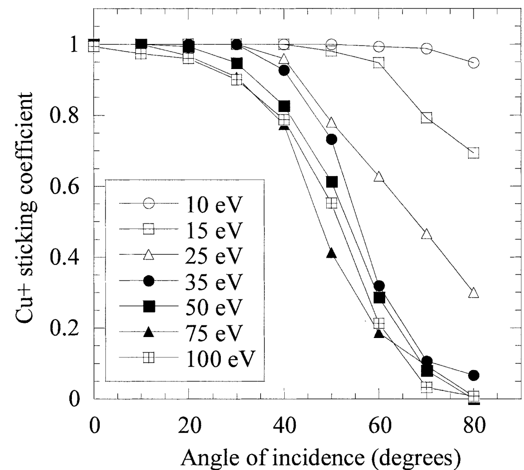

Fig. 4. Sticking coefficients for Cu^{+}/Cu amorphous surface (see text).

the smooth (111) surface results. On an amorphous surface, an ion may scatter off a protrusion and desorb. This is probably the reason why there is no upturn of sticking coefficients in the amorphous surface case. Also, the local impact angle on a roughened surface (measured with respect to local surface normal) will not necessarily be the same as the angle of incidence (measured with respect to the surface normal). These calculations show that the surface condition should have a large effect on the sticking coefficient at near grazing incidence for ion energies at intermediate range (10–50 eV). This result has also been observed in MD simulations of Cu [16] and Al [13] sputtering.

Considering all the factors above, one reasonable approach is to take the smooth surface results at low incidence angles and to incorporate the amorphous surface results at near grazing incidence angles. We took

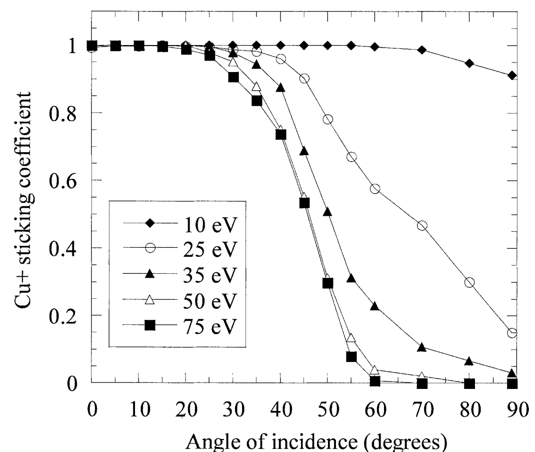

Fig. 5. The sticking coefficient curves for Cu^{+} as a function of angle and energy obtained by combining the crystalline and amorphous results (see text).

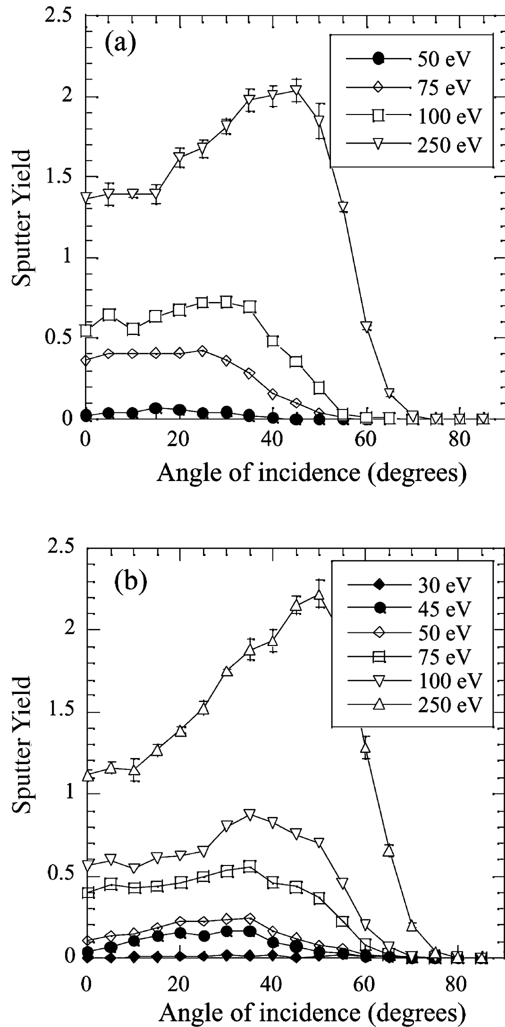

Fig. 6. (a) Sputter yield as a function of angle and energy for Ar^+ impacting a Cu(111) surface; error bars are shown for the 250 eV case. (b) Sputter yield as a function of angle and energy for Cu^+ impacting a Cu(111) surface, error bars are shown for the 250 eV case.

this approach in the Cu^+/Cu case and found that the connection between the two sets of data at incidence angles between 60° and 70° is reasonably smooth. Fig. 5 shows the combined sticking coefficient results after integration. We think that this result reflects a good description of the ion surface interaction in IMP Cu PVD conditions.

3.2. Sputter yield

Fig. 6a,b shows the sputter yield as a function of incidence angles for Ar^+ and Cu^+ impacting Cu(111) surfaces. The results shown in Fig. 6a,b are slightly different from our earlier results [12]. For a given ion energy, the maximum of sputter yield occurred at approximately 35° for low ion energies and gradually shifted towards approximately 50° as the ion energy increased. We also noticed that only the top surface atoms were sputtered in our MD simulations. This is in agreement with earlier theoretical conclusions that sputtering is mainly the result of collisions near the surface [24,25].

Fig. 7a,b show simulated normal incidence sputter yield as a function of ion energy for Ar^+ and Cu^+, a commonly used empirical formula [26], and experimental data [27]. The empirical formula is based on a fit to available experimental data. Given the fact that most of experimental data sets in the fitting database are at higher ion energies, the agreement between MD simulation and empirical formula is reasonable.

3.3. Thermal accommodation coefficient

The thermal accommodation coefficient (TAC) is a measure of the fraction of energy the incident atom deposits into the substrate. Fig. 8a,b shows the TAC as a function of incidence angle for Ar^+ and Cu^+ impacting a Cu(111) surface at different ion energies.

For Ar^+ impacting a Cu(111) surface, the TAC obeys a smooth curve that decreases as incidence angle increases. At near grazing incidence, the TAC approaches zero for all energies. The TAC is also larger for higher ion

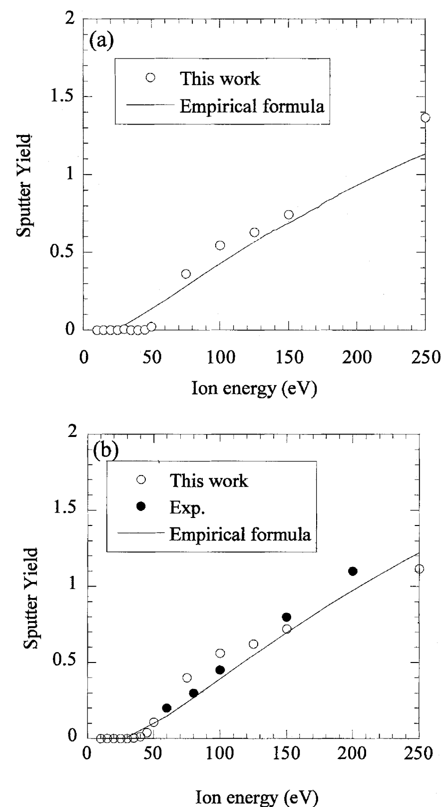

Fig. 7. (a) Sputter yield at normal incidence for Ar^+ ion impacting a Cu(111) surface and an empirical formula [27]. (b) Sputter yield at normal incidence for Cu^+ impacting a Cu(111) surface, experimental data [26], and an empirical formula [27].

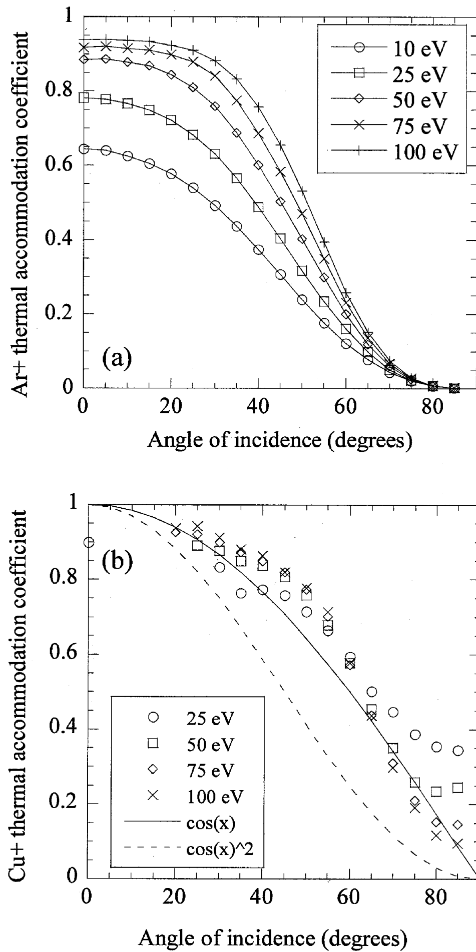

Fig. 8. (a) Thermal accommodation coefficient of Ar^+ impacting a Cu(111) surface as a function of angle and energy. (b) Thermal accommodation coefficient of Cu^+ impacting a Cu(111) surface as a function of angle and energy.

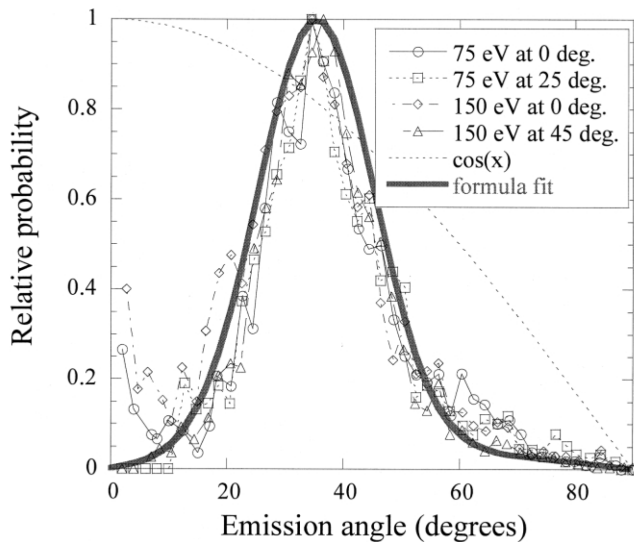

Fig. 9. Differential yield of sputtered Cu atoms for Ar^+ impacting Cu(111) surfaces.

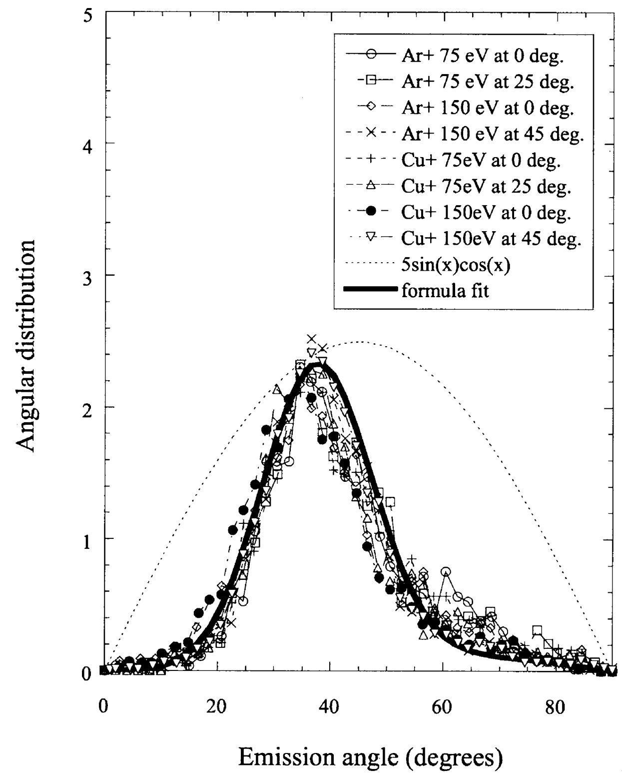

Fig. 10. Angular distributions (with solid angle factor) of sputtered Cu atoms for Ar^+ and Cu^+ impacting Cu(111) surfaces. The sputter distributions were scaled to have total sputter yield (the area under the sputter distribution curve) equal to that of cosine distribution ($=180/\pi$). The $\sin(\theta)\cos(\theta)$ function is scaled by a factor of 5.

energies, and approaches unity at normal incidence for a 100 eV Ar ion.

The data in the plots of TAC for Cu^+ impacting a Cu(111) surface are more scattered, but can be fit approximately to $\cos(\theta)$. In contrast, the TAC for Ar^+ impacting a Cu(111) surface has the shape of $\cos^2(\theta)$. The different behavior of the TAC between the Cu^+/Cu(111) and Ar^+/Cu(111) is probably due to the fact that Cu^+/Cu(111) has an attraction interaction. The Cu ion experiences a potential well of ~2 eV while Ar^+/Cu(111) is purely repulsive.

3.4. Angular distribution of sputtered particles

In feature scale deposition modeling, the sputtered atoms are usually assumed to have a cosine angular distribution about the surface normal [28,29],

$$f(\theta)=Y_0\cos(\theta) \tag{1}$$

where θ is the polar angle between the surface normal and the sputtered atom velocity direction, and Y_0 is a prefactor. The integral of $f(\theta)$ is the total sputter yield for a specified ion energy and incidence angle,

$$y(\theta)=c\int Y_0\cos(\theta)\sin(\theta)\mathrm{d}\theta\mathrm{d}\varphi \tag{2}$$

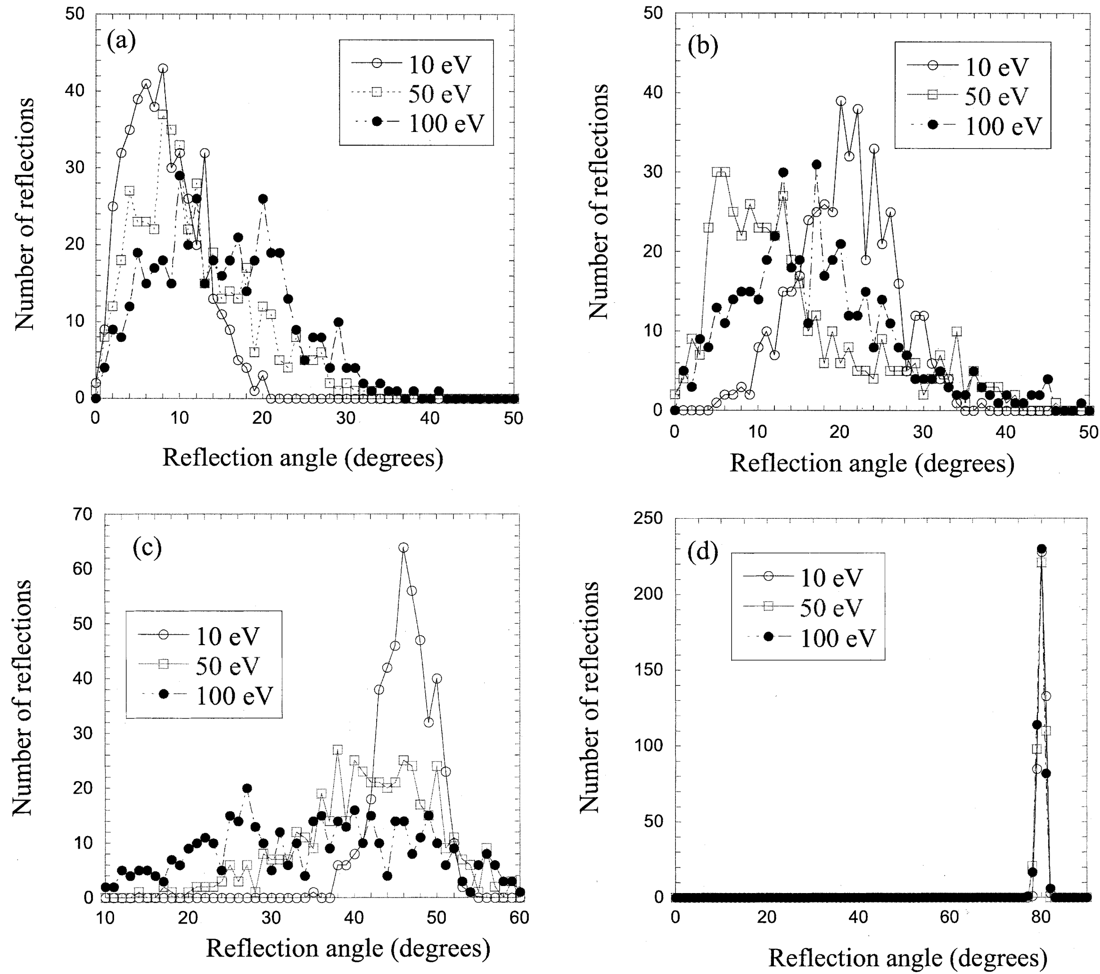

Fig. 11. Reflected ion angular distributions of Ar^+ impacting Cu(111) surface at 10 eV, 50 eV, and 100 eV at angles of incidence of (a) 0°, (b) 20°, (c) 45°, and (d) 80°.

where φ is the azimuthal angle and c is a normalization factor. The integration of the azimuthal angle φ can be separated, giving 2π. The integration factor, $\sin(\theta)d\theta d\varphi$ is also called the solid angle. $f(\theta)\sin(\theta)$ is a measure of the sputter yield at interval $d\theta$. $f(\theta)$, which is referred to as the differential yield or angular emission distribution (without solid angle factor), is obtained by the sputter yield at interval $d\theta$ divided by the $\sin(\theta)$ factor.

Fig. 9 shows the sputtered Cu atoms differential yield obtained from MD simulations for Ar^+ impacting Cu(111) surfaces at 75 eV and 150 eV ion energies, at angles of incidence of 0°, 25°, and 45°. The sputter distribution for each energy was normalized to unity for the highest value. For emission angles near zero, since $1/\sin(\theta)$ is a large value, small statistical error of the sputter yield determined from MD simulations results in very high statistical 'noise', as shown in Fig. 9. The final shapes of all sputter distributions peak close to 35° instead of at the surface normal, contrary to the cosine angular distribution.

We find that the narrow distribution shapes can be well described by a fit to a Gaussian-like formula centered close to 35.3° (see Fig. 9). The fitted angular emission (without solid angle) is

$$A\{0.967e^{[-((\theta-35.3)/10)^2/2]}+0.102\theta\cos(\theta)/90\} \qquad (3)$$

where $A=0.037942$ and θ is the emission angle.

In Fig. 10, additional MD results of Cu^+/Cu(111) sputter distributions at interval $d\theta$ with solid angle factor are shown, together with that for Ar^+/Cu(111). The sputter yield distributions were compared with that predicted by a cosine distribution [i.e. $\cos(\theta)\sin(\theta)$]. Both the shape and the location of the maximum differ. The Gaussian-like formula from Fig. 9 (multiplied by the solid angle factor) agrees with the Cu^+/Cu(111) sputter distribution results. To further verify this, we have also calculated: the sputter distributions of Ar^+ impacting a Cu(111) surface with ion energies from 75 to 150 eV, incidence angles from 0° to 50°; and, Cu^+ impacting a Cu(111) surface with ion energies from 50

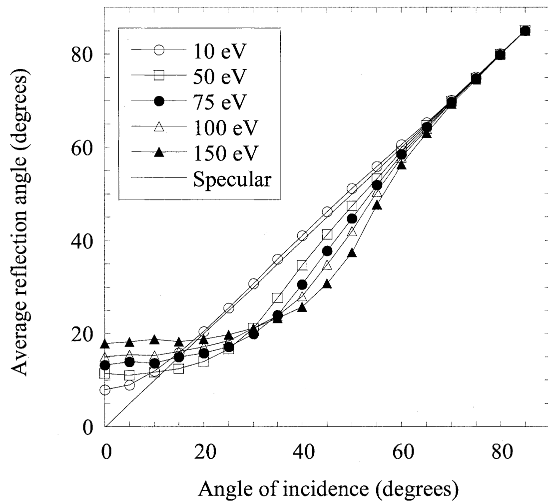

Fig. 12. Average reflection angle for Ar^+ impacting Cu(111) surface as a function of incidence angle. Pure specular reflection is shown by the solid line.

to 150 eV, incidence angles from 0° to 60° (for higher incidence angles, the sputter yield is very small). The sputtered particle distribution for Ar^+ or Cu^+/Cu(111) is found to be independent of incident ion energies or the angles of incidence considered.

Doughty et al. [30] have reported experimental results for the spatial distribution of Cu atoms sputtered by noble gas ions for ion energies in the range of 55 to 600 eV. They found that the distributions could not be described by a cosine distribution about the surface normal. Similar results were also reported in MD simulations of Ar^+/amorphous Cu surface [15]. The anisotropy in the angular distributions of particles ejected from keV ion-bombarded single-crystal surfaces was first observed by Wehner [31]. Another experimental study on angular distribution of atoms sputtered from polycrystalline metal targets concluded that atoms are ejected preferentially in the directions of their closest lattice neighbors [32]. Our findings are consistent with these observations. For both Ar^+ and Cu^+ on Cu(111) surfaces, the sputter differential yield distribution peaks close to 35.3°, which is the angle of the lattice neighbor direction ([110] in (111) surface). It is expected that maximum momentum transfer would occur along these directions during the initial collisions following ion impact.

3.5. Angular distribution of reflected ions

For Ar^+ impacting a Cu(111) surface at energies less than 100 eV, we find that all ions are reflected and the angular distribution varies with both the incident energy and angle. Fig. 11a–d show the angular distributions for Ar^+ at 10 eV, 50 eV, and 100 eV, with angles of incidence 0°, 20°, 45°, and 80°. At 80°, which is essentially grazing incidence, the reflection is specular. At lower angles, the distributions are broad peaks. Nevertheless, at zero angle of incidence, the distributions are at non-zero angle, with maxima between 7° and 20° depending on the ion energy. The average reflection angles for the Ar^+ are plotted in Fig. 12. The average reflection angles deviate from the specular values for ions with energy of 50 eV or higher at incidence angles from 0° to 60°. The deviations from specular turn from negative to positive at angles of ~20°. For ions with energy of 10 eV, the average reflection angle is nearly specular for most incidence angles except below 10°.

For Cu^+ impacting a Cu(111) surface, Cu ions tend to reflect if incidence angles are more than or equal to 20°. The Cu^+ reflection angular distribution is very different from that of Ar^+. Fig. 13 shows the average reflection angles for Cu^+ at 100 eV. The major difference compared with the Ar^+ case is that the Cu ions are emitted at high angles (with distribution average > 59°).

4. Conclusion

We performed MD simulations to study ion solid surface interactions relevant to IMP Cu PVD. Results for Ar^+/Cu(111) and Cu^+/Cu(111) as a function of ion energy and angle of incidence are presented. Besides sticking coefficients and sputter yields, we determined the angular distributions of sputtered and reflected particles, and thermal accommodation coefficients. For Cu^+ ions impacting an amorphous Cu surface, the sticking coefficient decreases monotonically with increasing angle of incidence. This is different from the crystalline Cu(111) surface results, which show a pronounced upturn near grazing incidence angles. The issue of integrating different sticking coefficients for different

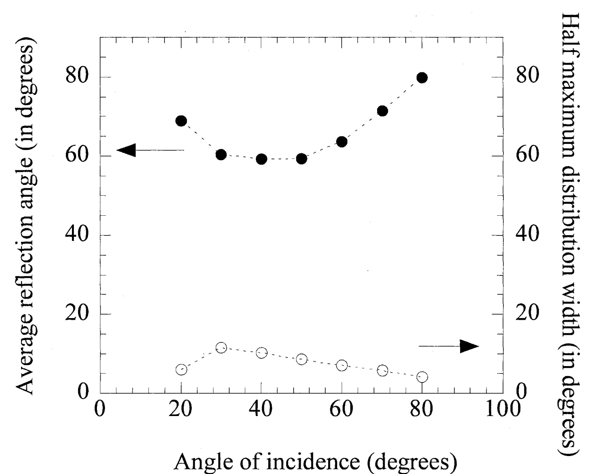

Fig. 13. Average reflection angle and the corresponding half maximum distribution width of 100 eV Cu^+ impacting Cu(111) surface as a function of incidence angle.

surface roughness was addressed, based on ion-travel-distance analysis. In this study, we also found that for $Ar^+/Cu^+/Cu(111)$ surface sputtering, the sputtered particle differential yield distributions are not cosine, but a narrow distribution with the peak close to the close-packed $\langle 110 \rangle$ direction for a $\{111\}$ surface in fcc crystal. This distribution is found to be independent of incident energy or angle. A simple Gaussian-like formula was found to describe the distribution well.

Acknowledgments

We would like to thank Michael Masquelier and Bill Johnson at Motorola for encouragement during the course of the work. We gratefully acknowledge useful discussions with Peter Ventzek at Motorola. We thank Cameron Abrams and David Graves at UC Berkeley for sharing their amorphous Cu surface coordinates with us. The work at Los Alamos National Laboratory (LANL) was carried out under the auspices of the US Department of Energy under Contract No. W-7405-ENG-36. This work was also supported by a Cooperative Research and Development Agreement (CRADA) 'Center for Semiconductor Modeling and Simulation' between the US Department of Energy and the Semiconductor Research Corporation and by a CRADA between LANL and Motorola, Inc.

References

[1] V. Arunachalam, D.G. Coronell, P.L.G. Ventzek, S. Rauf, M. Hartig, M.S. Daw, X.-Y. Liu, D. Denning, S. Garcia, Proceedings of Symposium on Dry Process, November 11–12, Tokyo, Japan, 1999, p. 63.

[2] V. Arunachalam, S. Rauf, D.G. Coronell, P.L.G. Ventzek, J. Appl. Phys. 90 (2001) 64.

[3] P.F. Cheng, S.M. Rossnagel, D.N. Ruzic, J. Vac. Sci. Technol. B 13 (1995) 203.

[4] S.M. Rossnagel, J. Vac. Sci. Technol. B 16 (1998) 2585.

[5] D.G. Coronell, D.E. Hansen, A.F. Voter, C.-L. Liu, X.-Y. Liu, J.D. Kress, Appl. Phys. Lett. 73 (1998) 3860.

[6] H. Feil, J. van Zwol, S.T. de Zwart, J. Dieleman, Phys. Rev. B. 43 (1991) 13695.

[7] M.H. Shapiro, T.A. Tombrello, Nucl. Instrum. Methods B 18 (1987) 355.

[8] H. Gades, H.M. Urbassek, Appl. Phys. A 61 (1995) 39.

[9] N.A. Kubota, D.J. Economou, S.J. Plimpton, J. Appl. Phys. 83 (1998) 4055.

[10] C.F. Abrams, D.B. Graves, J. Vac. Sci. Technol. A 16 (1998) 3006.

[11] R.A. McCoy, Ph.D. Thesis, The State University of New York at Stony Brook, 1995.

[12] J.D. Kress, D.E. Hanson, A.F. Voter, C.-L. Liu, X.-Y. Liu, D.G. Coronell, J. Vac. Sci. Technol. A 17 (1999) 2819.

[13] D.E. Hanson, B.C. Stephens, C. Saravanan, J.D. Kress, J. Vac. Sci. Technol. A 19 (2001) 820.

[14] D.E. Hanson, J.D. Kress, A.F. Voter, X.-Y. Liu, Phys. Rev. B 60 (1999) 11723.

[15] C.F. Abrams, D.B. Graves, IEEE Trans. Plasma Sci. 27 (1999) 1426.

[16] C.F. Abrams, D.B. Graves, J. Appl. Phys. 86 (1999) 2263.

[17] U. Hansen, P. Vogl, V. Fiorentini, Phys. Rev. B 59 (1999) R7856.

[18] U. Hansen, S. Rodgers, K.F. Jensen, Phys. Rev. B 62 (2000) 2869.

[19] A.F. Voter, Phys. Rev. B. 57 (1998) 13985.

[20] J.F. Ziegler, J.P. Biersack, U. Littmark, The Stopping and Ranges on Ions in Matter, Pergamon, New York, 1985.

[21] I.M. Torrens, Interatomic Potentials, Academic Press, New York, 1972.

[22] G.A. Kimmel, B.H. Cooper, Phys. Rev. B 48 (1993) 12164.

[23] D.E. Hanson, A.F. Voter, J.D. Kress, J. Appl. Phys. 82 (1997) 3552.

[24] D.E. Harrison, N.S. Levy, J.P. Johnson, H.M. Efron, J. Appl. Phys. 39 (1968) 3742.

[25] C. Lehmann, P. Sigmund, Phys. Stat. Sol. 16 (1966) 507.

[26] N. Matsunami, Y. Yamamura, Y. Itikawa, N. Itoh, Y. Kazuma, S. Miyagawa, K. Morita, R. Shimizu, H. Tawara, Atomic Data Nucl. Data Tables 31 (1984) 1.

[27] W.H. Hayward, A.R. Wolter, J. Appl. Phys. 40 (1969) 2911.

[28] S. Hamaguchi, S.M. Rossnagel, J. Vac. Sci. Technol. B 14 (1996) 2603.

[29] S. Hamaguchi, A.A. Mayo, S.M. Rossnagel, D.E. Kotecki, K.R. Milkove, C. Wang, C.E. Farrell, Jpn. J. Appl. Phys. 36 (1997) 4762.

[30] C. Doughty, S.M. Gorbatkin, L.A. Berry, J. Appl. Phys. 84 (1997) 1868.

[31] G.K. Wehner, J. Appl. Phys. Phys. 26 (1955) 1056.

[32] H. Tsuge, S. Esho, J. Appl. Phys. 52 (1981) 4391.